Photooxidation of Trp-191 in Cytochrome *c* Peroxidase by Ruthenium−Cytochrome *c* Derivatives†

Rui-Qin Liu,‡ Seung Hahm,‡ Mark Miller,§ Bill Durham,‡ and Francis Millett*,‡

Department of Chemistry and Biochemistry, University of Arkansas, Fayetteville, Arkansas 72701, and Department of Chemistry, University of California at San Diego, La Jolla, California 92093

Received August 9, 1994; Revised Manuscript Received November 14, 1994®

ABSTRACT: A novel photoinduced electron-transfer reaction is reported in complexes between resting ferric state cytochrome *c* peroxidase (CcP) and several horse cytochrome *c* derivatives labeled at single lysine amino groups with [bis(bipyridine)](dicarboxybipyridine)ruthenium(II) (Ru-CC). Photoexcitation of Ru(II) in the 1:1 Ru-27-CC:CcP complex results in formation of a metal-to-ligand charge-transfer state, Ru(II*), which is a strong reducing agent and rapidly transfers an electron to the CC heme Fe(III) with rate constant $k_1 = 2.3 \times 10^7$ s^{-1}. The resulting Ru(III) is a strong oxidizing agent with a redox potential of 1.3 V, and it oxidizes the indole ring of Trp-191 with rate constant $k_3 = 7 \times 10^6$ s^{-1}. The cycle is completed by electron transfer from Fe(II) in CC to the Trp-191 radical in CcP with rate constant $k_4 = 6.1 \times 10^4$ s^{-1}. The Ru group is located close to the interaction domain in the Ru-27-CC:CcP complex, allowing rapid electron transfer with both the heme in CC and Trp-191 in CcP. The electron-transfer reaction was not observed in CcP compound I, where Trp-191 is already oxidized to the radical, or in the W191F mutant, where the indole group is replaced with a phenyl group. The electron-transfer reaction was observed in CcP mutants modified at residues in the heme crevice, R48K, R48L, H52L, M230I, and M231I, but not in D235N which destabilizes the radical on Trp-191. Increasing the ionic strength results in an increase in the equilibrium dissociation constant K of the Ru-27-CC:CcP complex and an increase in the rate constant k_5 for dissociation of the transient intermediate containing Fe(II) CC and the radical form of CcP. Both K and k_5 were also increased significantly by the mutations D34N, E290N, and A193F involving residues located in the interaction domain of the crystalline complex between yeast CC and CcP [Pelletier & Kraut (1992) *Science 258,* 1748−1755]. This new method allows the study of the electron-transfer reaction between CC and the radical on Trp-191 in the complete absence of hydrogen peroxide, and it opens the possibility of measurements at low temperatures in frozen glasses or in crystals.

The reaction between cytochrome *c* and cytochrome *c* peroxidase is a unique system for the study of long-range inter-protein electron transfer because of the extensive structural characterization of the individual proteins as well as of their 1:1 complex (Finzel et al., 1984; Louie & Brayer, 1990; Pelletier & Kraut, 1992). In the first step of the reaction, the resting ferric state of cytochrome *c* peroxidase, CcP,[1] is oxidized by hydrogen peroxide to compound I, CMPI(IV,R•), in which the two oxidized sites are the oxyferryl heme Fe(IV)=O and a protein-based radical (Yonetani et al., 1966; Coulson et al., 1971). Extensive studies utilizing ENDOR, EPR, and mutagenesis techniques established that the radical is located on the indole group of Trp-191 (Mauro et al., 1988; Scholes et al., 1989; Erman et al., 1989; Sivaraja et al., 1989; Fishel et al., 1991; Goodin et al., 1987). The orientation of Trp-191 is maintained by a hydrogen bond network linking Trp-191, Asp-235, and His-175, the proximal heme ligand (Wang et al., 1990). Miller et al. (1994a) have recently identified a strong cation binding site in the cavity formerly occupied by the side chain of Trp-191 in a CcP mutant in which Trp-191 is replaced with Gly. They propose that the radical on Trp-191 is a cation indolyl radical that is stabilized by the backbone carbonyl oxygen atoms of residues 175 and 177, as well as the heme propionates and the carboxylate side chain of Asp-235. Houseman et al. (1993) have recently reported that the anomalous EPR spectrum of the radical in CMPI is due to a weak exchange interaction between the radical on Trp-191 and the S = 1 Fe(IV)=O center.

The mechanism of reduction of CMPI by ferrocytochrome *c* [CC(II)] has been studied extensively (Coulson et al., 1971; Hazzard et al., 1987, 1988a−c; Hazzard & Tollin, 1991; Summers & Erman, 1988). Geren et al. (1991) and Hahm et al. (1992) found that a wide variety of ruthenium-labeled horse and yeast cytochrome *c* derivatives first reduced the radical in CMPI(IV,R•) to form CMPII(IV,R). At low ionic strength where a stable complex is formed between the two proteins, the rate constant for the intracomplex reaction is 50 000 s^{-1} or larger, depending on the ruthenium cytochrome *c* (Ru-CC) derivative. As ionic strength is increased, the complex dissociates and second-order kinetics are observed, but the radical remains the initial site of reduction in CMPI (Geren et al., 1991; Hahm et al., 1992; Liu et al., 1994). Both native horse and yeast CC(II) initially reduce the radical in CMPI at high ionic strength where the reaction is slow enough to resolve by stopped-flow spectroscopy (Hahm et

† This work was supported in part by NIH Grant GM20488 to B.D. and F.M. and NSF Grant MCB 9119292 to M.M. and J.K.

‡ University of Arkansas.

§ University of California at San Diego.

® Abstract published in *Advance ACS Abstracts,* January 1, 1995.

[1] Abbreviations: CcP, cytochrome *c* peroxidase; hCC, horse cytochrome *c*; yCC, yeast iso-1-cytochrome *c*; Ru-27-CC, [bis(bipyridine]-(4,4′-dicarboxybipyridine−Lys-27-cytochrome *c*)ruthenium(II).

0006-2960/95/0434-973$09.00/0

Scheme 1

$$\text{CMPI(IV,R}^{\bullet}) + \text{CC(II)} \rightarrow \text{CMPII(IV,R)} + \text{CC(III)} \quad (1)$$

$$\text{CMPII(IV,R)} \rightleftarrows \text{CMPII(III,R}^{\bullet}) \quad (2)$$

$$\text{CMPII(III,R}^{\bullet}) + \text{CC(II)} \rightarrow \text{CcP(III,R)} + \text{CC(III)} \quad (3)$$

Scheme 2

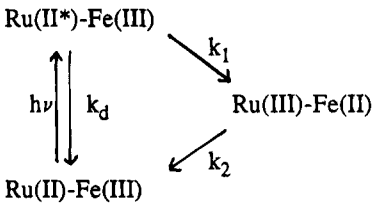

al., 1993, 1994; Miller et al., 1994b; Nuevo et al., 1993). When the ionic strength is reduced to 5 mM, the reaction between equimolar horse or yeast CC(II) and the radical in CMPI becomes too fast to measure by stopped-flow spectroscopy (Hahm et al., 1993, 1994; Erman et al., 1993; Summers & Erman, 1988; Miller et al., 1994b). A mechanism involving rapid reduction of the radical in CMPI by CC(II) is consistent with the electron-transfer pathway proposed by Pelletier and Kraut (1992) on the basis of the crystal structure of the 1:1 complex between yeast iso-1-CC and CcP. This pathway extends from the exposed heme CBC methyl group of CC through CcP residues Ala-194, Ala-193, and Gly-192 to the indole group of Trp-191.

Liu et al. (1994) have recently shown that reduction of the CMPI radical on Trp-191 is followed by intramolecular electron transfer from Trp-191 to the Fe(IV) center of CMPII (reaction 2 of Scheme 1). The pH dependence of the extent and rate of reaction 2 is correlated with the rate of reduction of the Fe(IV)=O center by excess CC(II), providing experimental support for Scheme 1. In this mechanism, both interprotein reactions would utilize a common electron-transfer pathway and a common interaction domain. This is supported by recent mutagenesis experiments (Miller et al., 1994b) demonstrating that the Pelletier−Kraut interaction domain is utilized for reduction of both the radical and the Fe(IV)=O center by CC(II). Support for Scheme 1 is based largely on experiments carried out under conditions where only a single molecule of CC(II) binds to CMPI at a time. It is possible that direct reduction of Fe(IV)=O might occur at low ionic strength through a second low-affinity CC(II) binding site as suggested by the experiments of Stemp and Hoffman (1993), Zhou and Hoffman (1993, 1994), and Summers and Erman (1988).

In the present paper we report a novel photoinduced electron-transfer reaction in complexes between resting state CcP and several CC derivatives labeled at single lysine amino groups with [bis(bipyridine)](dicarboxybipryidine)ruthenium-(II) [Ru(II)]. Photoexcitation of Ru(II) in Ru-CC results in formation of a metal-to-ligand charge-transfer state, Ru(II*), which is a strong reducing agent and rapidly transfers an electron to heme Fe(III) with rate constant k_1 as shown in Scheme 2. The resulting Ru(III) is a strong oxidizing agent with a redox potential of 1.3 V for the Ru(III)/Ru(II) couple, and it oxidizes heme Fe(II) with rate constant k_2. In studies of inter-protein electron transfer between Ru-CC and CMPI, a sacrificial electron donor such as EDTA or aniline is used to reduce Ru(III) and prevent the back reaction (Geren et al., 1991; Hahm et al., 1992). However, it was discovered that photoexcitation of a complex between resting state CcP and Ru-CC in the absence of a sacrificial donor resulted in reduction of the heme Fe(III) of Ru-CC by Ru(II*), followed by oxidation of the indole ring of Trp-191 by Ru(III) (Scheme 3). The cycle is completed by electron transfer from Fe(II) to the Trp-191 radical. This technique is developed in the present paper to characterize the electron-transfer properties of the indolyl radical on Trp-191 using a wide range of CcP mutants.

Scheme 3

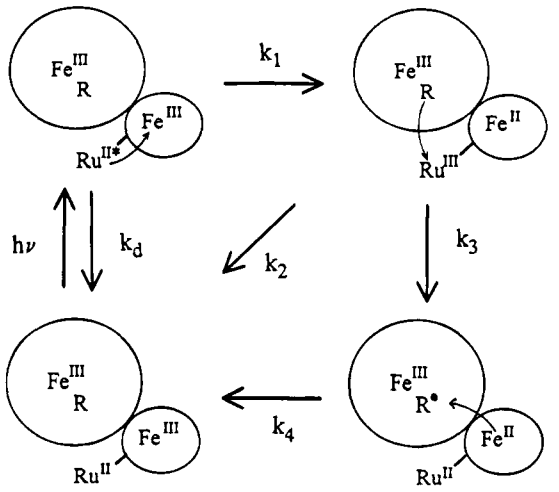

EXPERIMENTAL PROCEDURES

Materials. Ru-CC derivatives labeled at single lysine amino groups with (dicarboxybipyridine)[bis(bipyridine)]-ruthenium(II) were prepared and characterized as described by Pan et al. (1988) and Durham et al. (1989), while Ru_m-CC derivatives modified with (dimethylbipyridine)[bis-(bipyridine)]ruthenium(II) were prepared and characterized as described by Geren et al. (1991) and Pan et al. (1993). The parent enzyme CcP(MI) and the mutants W191F, M230I, M231L, R48K, R48L, H52L, D235N, Y39F, Y42F, H181G, W223F, Y229F, E32Q, D34N, E35Q, E290N, E291Q, and A193F were prepared and characterized as described by Fishel et al. (1987, 1991) and Miller et al. (1988, 1994b).

Transient Absorbance Measurements. Flash photolysis experiments were carried out with two different instruments for fast and slow time domains. For fast kinetic studies with a time domain up to 5 μs, the excitation pulse was the third harmonic of a Nd:YAG laser with a pulse width of 20 ns and a wavelength of 356 nm. A pulsed 75-W xenon arc lamp was used as the probe source as described by Durham et al. (1989). The monochromater was set to a band-pass of 1.5 nm, and the photomultiplier detector had a response time of 10 ns. For longer time domains, from 5 μs up to 1 s, a Phase R Model DL 1400 flashlamp-pumped dye laser using coumarin 450 to produce a 450-nm light pulse of <0.5-μs duration was used as the excitation source. The monochromater was set to 1.5-nm band-pass, and the photomultiplier detector had a response time of 1 μs. For some experiments, a high-sensitivity detector utilizing 10 nm band-pass interference filters was used as described by Pan et al. (1993). The transient signal was recorded with a LeCroy 7200 digitizer at a maximum resolution of 1 ns per point and transferred to a 486 personal computer for analysis. The

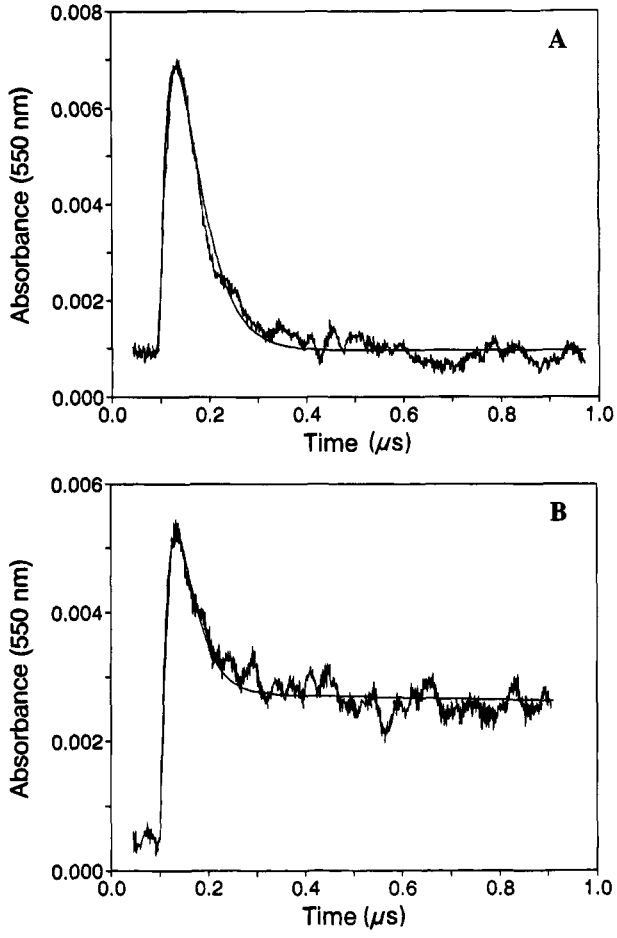

FIGURE 1: Photoinduced electron transfer in complex between Ru-27-CC and CcP. (A) A solution containing 10 μM Ru-27-CC in 2 mM sodium phosphate, pH 6, was excited with a 25-ns laser flash at 355 nm. Transients were recorded at 550, 556.5, and 434 nm. The 550-nm transient shown indicates formation and decay of Fe(II). The smooth line is the best fit to Scheme 2, with $k_1 = 2.3 \times 10^7$, $k_2 = 2.2 \times 10^7$, and $k_d = 2.1 \times 10^7$ s^{-1}. (B) A solution containing 10 μM Ru-27-CC and 10 μM CcP in 2 mM phosphate, pH 6, was excited with a laser flash under the same conditions as in (A). The smooth line is the best fit to Scheme 3 with $k_1 = 2.3 \times 10^7$, $k_2 = 2.2 \times 10^7$, $k_d = 2.1 \times 10^7$, $k_3 = 7.5 \times 10^6$, and $k_4 = 6.1 \times 10^4$ s^{-1}.

experimental transients of the Ru-CC derivatives were fit with the equations given by Durham et al. (1989) to find the values of k_1, k_2, and k_d shown in Scheme 2. The experimental transients for the complex between Ru-CC and CcP were fit to the mechanism shown in Scheme 3 by numerical integration methods (Strickland et al., 1975). The flash photolysis experiments were carried out in glass semimicro cuvettes containing 300-μL solutions of 2 mM sodium phosphate, pH 6, 3−10 μM Ru-CC, and 0−20 μM CcP.

RESULTS

Photoinduced Electron Transfer in Ru-CC:CcP Complexes. Flash photolysis of a solution containing 10 μM Ru-27-CC in 2 mM sodium phosphate, pH 6, with the YAG laser resulted in electron transfer from Ru(II*) to Fe(III), followed by the thermal back reaction from Fe(II) to Ru(III) as shown in Scheme 2. The reduction and reoxidation of the CC heme were measured at 550 nm (Figure 1A), while the photoexcitation and recovery of Ru(II) were measured at 434 nm, an isosbestic for CC. Ru(II*) and Ru(III) do not contribute significantly to the absorbance at 434 nm. The luminescence decay rate of Ru(II*) was found to be 4.4×10^7 s^{-1}, which defines the value of $k_1 + k_d$. A unique set of values for k_1, k_2, and k_d were needed in order to simultaneously fit the 550-nm transient, the 434-nm transient, and the luminescence decay rate, using the equations and procedures given by Durham et al. (1989). The rate constants were found to be $k_1 = 2.3 \times 10^7$, $k_2 = 2.2 \times 10^7$, and $k_d = 2.1 \times 10^7$ s^{-1}, with errors of ±15%. The values of the rate constants for the Ru-13-CC and Ru-72-CC derivatives are given in Table 1.

When 10 μM CcP was added to 10 μM Ru-27-CC, the magnitude of the 550-nm absorbance change corresponding to the rapid reoxidation of Fe(II) was decreased by about 50% (Figure 1B). No significant changes were observed in the 434-nm transient or the luminescence decay rate of Ru(II*). The reaction was measured on a longer time scale using the dye laser instrument, which has a response time of 1 μs. The rapid phase of reoxidation of Fe(II) is not resolved with this response time. The 550-nm transient indicated that the Fe(II) remaining 1 μs after the laser flash was oxidized with a rate constant of $k_4 = 6.1 \times 10^4$ s^{-1} (Figure 2A). Similar results were observed for complexes of Ru-13-CC and Ru-72-CC with CcP, with k_4 values of 5.2×10^3 and 1.4×10^4 s^{-1}, respectively (Table 1). The concentration dependence of the kinetics was consistent with electron transfer within a 1:1 Ru-CC:CcP complex with a dissociation constant of less than 1 μM for each of the Ru-CC derivatives. The amplitude of the 550-nm transient recorded with the dye laser instrument increased linearly as the concentration of CcP was increased from 0 to 5 μM at a constant Ru-72-CC concentration of 5.5 μM, and it then remained constant as the CcP concentration was increased to 20 μM (Figure 3). The rate constant k_4 was independent of CcP concentration from 1.5 to 20 μM. The fast transients observed in the YAG laser instrument were independent of CcP concentration as long is it was equal to or greater than that of Ru-CC.

Scheme 3 was investigated as a working hypothesis for the photoinduced electron-transfer kinetics in the Ru-CC:CcP complex. The photoexcited Ru(II*) transfers an electron to the CC heme Fe(III) to form Fe(II) and Ru(III). The strong oxidant Ru(III) then oxidizes the indole ring of Trp-191, resulting in formation of a radical. The cycle is completed by electron transfer from the Fe(II) in Ru-CC to the radical at Trp-191 of CcP. The 550-nm, 434-nm, and luminescence decay transients measured with the YAG laser instrument, as well as the 550-nm transient measured with the dye laser instrument, were simultaneously fitted to Scheme 3 using numerical integration techniques. This fitting procedure resulted in the following unique set of rate constants for the Ru-27-CC:CcP complex: $k_1 = 2.0 \times 10^7$, $k_d = 2.4 \times 10^7$, $k_2 = 2.4 \times 10^7$, $k_3 = 7 \times 10^6$, and $k_4 = 6.1 \times 10^4$ s^{-1}, all with errors of ±20%. Note that according to this scheme, the oxidation of Trp-191 by Ru(III) is competitive with the oxidation of Fe(II) by Ru(III). The yield of the intermediate state CC(II):CMPII(III,R$^\bullet$) is relatively small since the value of k_3 is smaller than that of k_2. The results for the complexes involving Ru-13-CC and Ru-72-CC were also fitted to Scheme 3 with the rate constants given in Table 1. A number of experiments were carried out to test Scheme 3.

Table 1: Photoinduced Electron Transfer in Ru-CC:CcP Complexes[a]

Ru-CC	CcP	k_1 ($\times 10^7$ s^{-1})	k_2 ($\times 10^7$ s^{-1})	k_d ($\times 10^7$ s^{-1})	k_3 ($\times 10^7$ s^{-1})	k_4 ($\times 10^4$ s^{-1})
Ru-27-CC		2.3	2.2	2.1		
Ru-27-CC	CcP	2.0	2.4	2.4	0.7	6.1
Ru-27-CC	CMPI	2.1	2.3	2.0	0	0
Ru-27-CC	CcP(W191F)	2.5	2.4	2.2	0	0
Ru-13-CC		1.6	2.6	0.8		
Ru-13-CC	CcP	1.7	2.5	0.9	0.4	0.5
Ru-72-CC		1.6	2.3	1.0		
Ru-72-CC	CcP	1.5	2.2	1.1	0.2	1.4

[a] Solutions contained 5−10 μM Ru-CC and 0−20 μM CcP in 2 mM sodium phosphate, pH 6. Transients were recorded at 434, 550, and 556.5 nm in both the YAG laser instrument and the dye laser instrument. Ru(II*) fluorescence lifetimes were measured as described by Durham et al. (1989). The transients were simultaneously fitted to Scheme 2 as described by Durham et al. (1989) or to Scheme 3 using numerical integration methods (Hahm et al., 1994). k_1, k_2, k_3, and k_d were obtained from the YAG laser transients, while k_4 was obtained from the dye laser transients. The errors in each parameter are ±15%.

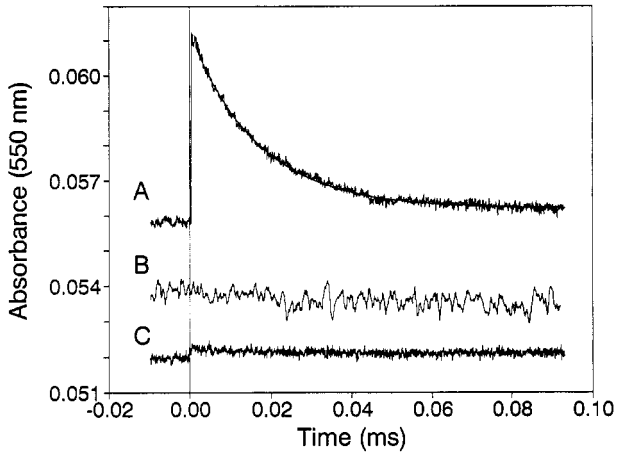

FIGURE 2: Photoinduced electron transfer in complex between Ru-27-CC and CcP. (A) A solution containing 5 μM Ru-27-CC and 5 μM CcP in 2 mM sodium phosphate, pH 6, was excited with a 0.3-μs, 450-nm light flash from the dye laser. The detection system had a response time of 1 μs, and the rapid reduction and reoxidation of Fe(II) in Ru-27-CC:CcP seen in Figure 1B were not resolved. The 550-nm transient shown is the average of 10 transients. The 550-nm transient was fit to a single exponential with $k_4 = 6.1 \times 10^4$ s^{-1}. (B) The solution in (A) was treated with 5 μM H_2O_2 to convert CcP to CMPI. Laser excitation under the same conditions as in (A) resulted in no transient absorbance changes. The signal shown is a single transient. (C) A solution containing 5 μM Ru-27-CC and 5 μM W191F CcP in 2 mM sodium phosphate was photoexcited as in (A). The 550-nm signal shown is the average of 10 transients.

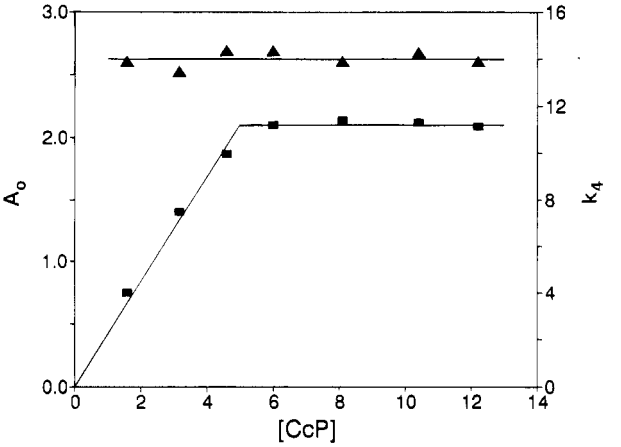

FIGURE 3: Concentration dependence of reaction between Ru-72-CC and CcP. Solutions containing 5.5 μM Ru-72-CC and 0−20 μM CcP in 2 mM sodium phosphate, pH 6, were photoexcited in the dye laser instrument. The values of A_o and k_4 were measured as a function of the concentration of CcP.

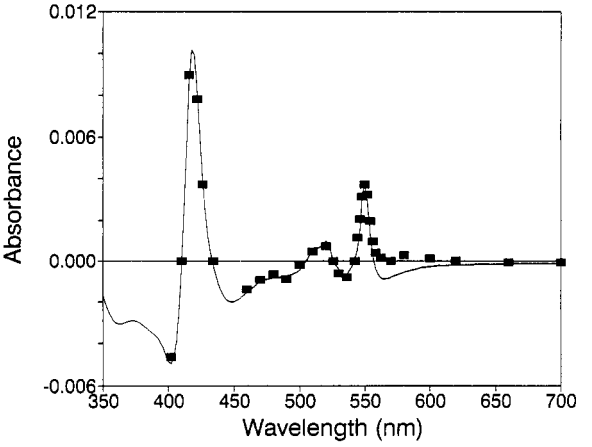

FIGURE 4: Wavelength dependence of the transient following photoexcitation of a complex between Ru-27-CC and CcP. A sample containing 10 μM Ru-27-CC and 10 μM CcP in 2 mM sodium phosphate, pH 6, was photoexcited in the dye laser instrument, and the absorbance change A_o 2 μs after the laser flash relative to the absorbance change immediately before the laser flash was measured as a function of wavelength. The points above 560 nm were measured in a high-sensitivity detector utilizing 10 nm band-pass interference filters.

Difference Spectrum for the Transient Intermediate in the Photoexcited Ru-CC:CcP Complex. The wavelength dependence of the absorbance change of the Ru-72-CC:CcP complex was measured 2 μs after the laser flash using the dye laser instrument. At this time the initial rapid electron-transfer reactions will be completed, and the final electron-transfer step will not have begun. The transient difference spectrum is in general agreement with the Fe(II) − Fe(III) difference spectrum for CC in the Soret region and the 460−560-nm region (Figure 4). This demonstrates that the CC heme has been reduced. There is no significant absorbance change at the CC isosbestic of 434 nm, indicating no oxidation of the CcP heme Fe(III) to an oxyferryl Fe(IV)=O state. However, a small absorbance increase was observed in the wavelength region 556−640 nm where the Fe(II) − Fe(III) difference spectrum for CC is negative. The absorbance change is very small and required a highly sensitive detector utilizing interference filters. The small positive absorbance in this wavelength region is similar to the difference spectrum for CMPI(IV,R•) − CMPII(IV,R) reported by Coulson et al. (1971) and Ho et al. (1983). However, no spectral properties for the species CMPII(III,R•) have been reported, and the CMPII(III,R•) − CcP(III,R)

difference spectrum is not necessarily the same as that of CMPI(IV,R•) − CMPII(IV,R). The transient difference spectrum is consistent with the identification of the transient intermediate as CC(II):CMPII(III,R•). The same absorbance difference spectrum was observed for the complexes involving Ru-13-CC and Ru-27-CC.

Effect of CMPI Formation on Intracomplex Electron Transfer with Ru-27-CC. A sample containing 5 μM Ru-27-CC and 5 μM CcP in 2 mM sodium phosphate, pH 6, was treated with 1 equiv (5 μM) of H_2O_2 to form the Ru-27-CC:CMPI(IV,R•) complex. The 550-nm transient observed in the YAG laser instrument was the same as that of Ru-27-CC alone (Figure 1A) and rapidly returned to the preflash baseline. The rate constants were nearly the same as that of uncomplexed Ru-27-CC (Table 1). No 550-nm transient at all was observed with the dye laser instrument for this complex under the same conditions used for studying the Ru-27-CC:CcP complex (Figure 2B). These results indicate that the photoreduced Fe(II) was completely reoxidized by Ru(III), and no other species in CMPI(IV,R•) reacted with Ru(III). This is consistent with Scheme 3, since the indole group of Trp-191 is already oxidized in CMPI-(IV,R•) and is not available to transfer an electron to Ru-(III).

Effect of Sacrificial Electron Donors on Photoinduced Electron Transfer in the Ru-27-CC:CcP Complex. Laser photoexcitation of a solution containing 10 mM aniline in addition to 5 μM Ru-27-CC and 6 μM CcP in 2 mM sodium phosphate, pH, 6 resulted in a rapid increase in absorbance at 550 nm, but no subsequent decrease in absorbance (Hahm et al., 1992). Similar results were obtained with other sacrificial electron donors such as EDTA. This result indicates that Ru(II*) rapidly reduces the heme in Ru-27-CC, and the resulting Ru(III) is then rapidly reduced by the sacrificial electron donor before it can oxidize Trp-191 or Fe(II). If 1 equiv of H_2O_2 was added to the above solution to form CMPI(IV,R•), then biphasic electron transfer from the photoreduced Fe(II) to the radical in CMPI(IV,R•) was observed, as previously reported (Hahm et al., 1992). The rate constant for the fast phase of this reaction, k_{etf}, is nearly the same as the rate constant k_4 obtained by photoexciting the Ru-27-CC:CcP complex in the absence of H_2O_2 and aniline (Table 2). These results provide support for Scheme 3, since k_4 represents electron transfer to the radical in CMPII(III,R•), while k_{etf} represents electron transfer to the radical in CMPI(IV,R•). The slow phase in the reduction of CMPI(IV,R•), k_{ets}, is not observed in the photoexcitation studies in the absence of H_2O_2 and aniline, consistent with the assignment of this phase to a nonproductive binding mode (Hahm et al., 1992).

Flash Photolysis of Ru-27-CC:CcP(MI,W191F) Complex. Flash photolysis of a solution containing 10 μM Ru-27-CC and 10 μM CcP(MI,W191F) in 2 mM sodium phosphate, pH 6, with the YAG laser instrument resulted in 550- and 434-nm transients that were essentially the same as those of Ru-27-CC alone (Table 1). The 550-nm transient rapidly returned to the preflash baseline, indicating that photoreduced Fe(II) was completely reoxidized by Ru(III), and no species in CcP(MI,W191F) reduced Ru(III). No 550-nm transient at all was observed with the dye laser instrument (Figure 2C). These results are consistent with Scheme 3, since a phenyl group could not be oxidized by Ru(III). X-ray crystallography has shown that the structure of CcP(W191F) is the same as that of the CcP parent except in the immediate vicinity of residue 191 (Wang et al., 1990). In order to verify that CcP(MI,W191F) formed a complex with Ru-27-CC, a competition experiment was carried out (Figure 5). Addition of increasing concentrations of CcP(MI,W191F) to a solution containing 5 μM Ru-27-CC and 5 μM CcP in 2 mM sodium

Table 2: Intracomplex Electron Transfer between Ru-CC and CcP Mutants[a]

CcP(MI) mutants	Ru-13-CC		Ru-27-CC		Ru-72-CC	
	k_4	k_{etf}	k_4	k_{etf}	k_4	k_{etf}
			Class A Mutants			
CcP(MI)	5.2	6.6	61	50	14	12
R48K	6.0	*	38	*	14	*
R48L	9.3	*	49	*	17	*
H52L	13	*	49	*	24	*
W191F	0	*	0	*	0	*
M230I	14	12	47	48	22	20
M231L	10	*	45	*	20	*
D235N	0	*	0	*	0	*
			Class B Mutants			
CcP(MI)	5.2	6.6	61	50	14	12
Y39F	10	6.0	56	46	22	16
Y42F	8.0	7.6	42	39	21	16
H181G	22	15	23	20	20	16
W223F			46	40	18	15
Y229F	11	11	31	35	18	18
			Class C Mutants			
CcP(MI)	5.2	6.6	61	50	14	12
E32Q	7.8	3.4	88	56	22	16
D34N	7.7	3.2	134	39	10	10
E35Q	2.3	2.1	88	32	13	15
E290N	4.4	3.5	40	23	10	11
E291Q	5.1	7.1	67	40	13	14
A193F	5.8	11	42	22	13	12

[a] Solutions containing 5−10 μM Ru-CC and 5−20 μM CcP mutants in 2 mM sodium phosphate were photoexcited in the dye laser instrument, and the rate constant k_4 of Scheme 3 was measured from the 550-nm transient. The rate constant k_{etf} for the fast phase of the reaction between Ru-CC and CMPI was determined under the same conditions as described by Hahm et al. (1992, 1994). The mutants for which CMPI was too unstable to measure k_{etf} are indicated by an asterisk (*). The k_{etf} data for the class B mutants came from Hahm et al. (1994), while the data for the class C mutants came from Miller et al. (1994b). The rate constants are in units of 10^3 s^{-1}, and the errors are ±15%.

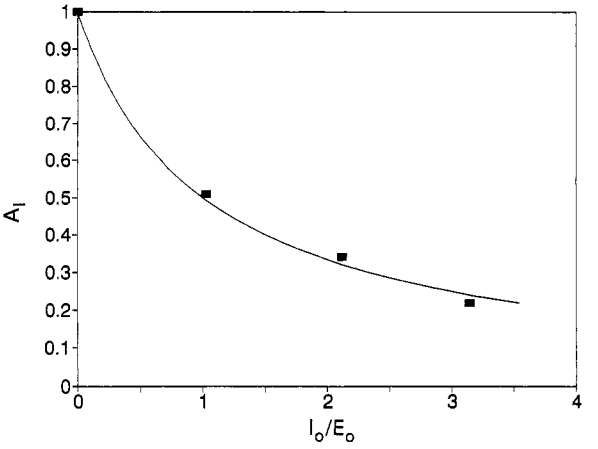

FIGURE 5: Effect of W191F CcP on photoinduced electron transfer between Ru-27-CC and CcP. A solution containing 5 μM Ru-27-CC, 5 μM CcP (E), and 0−15 μM CcP(W191F) (I) in 2 mM sodium phosphate, pH 7, was photoexcited in the dye laser instrument. The 550-nm absorbance increase A_o was measured 2 μs after the laser flash. A_I is the ratio of A_o measured in the presence of I relative to the value in the absence of I. The solid line is the best fit of the equation for mechanism 4 to the data, with $K_I/K_E = 1.0$.

phosphate, pH 6, resulted in a progressive decrease in the amplitude of the 550-nm transient due to electron transfer in the Ru-27-CC:CcP complex. This decrease in amplitude was analyzed in terms of the following competition between CcP(MI) (E) and CcP(MI,W191F) (I) for binding to Ru-27-CC (CC):

$$CC + E \rightleftharpoons CC{:}E \qquad CC + I \rightleftharpoons CC{:}I \qquad (4)$$

It was assumed that the transient is due entirely to the CC:E complex and that the dissociation constant K_E for the CC:E complex is <1 μM, as previously shown, so that the CC:E complex is fully formed in the absence of I. Under these conditions, the dissociation constant K_I for the CC:I complex will be given by

$$I_o/E_o = 1 - A_I + [(1 - A_I)^2/A_I](K_I/K_E)$$

where I_o and E_o are the total concentrations of I and E, and A_I is the amplitude of the transient in the presence of I relative to the amplitude in the absence of I. The best fit to the data of Figure 5 was obtained with $K_I/K_E = 1.0 \pm 0.2$. The results indicate that the W191F mutant binds to Ru-27-CC with the same affinity as the parent CcP.

Dependence of Photoinduced Electron Transfer in Ru-CC:CcP Complex on Position of Ru. The photoinduced inter-protein electron-transfer reaction was only observed in complexes between CcP and Ru-13-CC, Ru-27-CC, and Ru-72-CC (Table 1). The values of k_3 and k_4 were smaller for Ru-13-CC and Ru-72-CC than for Ru-27-CC. In each case, the value of k_4 was nearly the same as the value of k_{etf} (Table 2). No inter-protein photoinduced electron-transfer reactions were detected in complexes between CcP and Ru-CC derivatives labeled at lysine 8, 25, 39, 55, or 60. Lysines 13 and 72 are located within the Pelletier–Kraut binding domain, while lysine 27 is close to the binding domain. All of the other labeled lysines are remote from the binding domain on CC for CcP. These results indicate that the Ru label must be close to the CC:CcP binding interface.

Photoinduced Electron Transfer in Complexes between CcP Mutants and Ru-CC. The photoinduced electron-transfer reaction between the Ru-CC derivatives and a wide range of CcP mutants was examined (Table 2). These mutants fall into three different classes: (A) mutants that alter the heme crevice of CcP, (B) mutants that potentially affect the electron-transfer pathway, and (C) mutants that potentially affect complex formation. In class A, the D235N mutant had no detectable intracomplex electron-transfer reaction. This is consistent with the observation that Asp-235 forms a hydrogen bond with Trp-191 in the CcP parent, and mutation of Asp-235 to Asn prevents formation of the radical on the indole group of Trp-191. Thus, the absence of photoinduced electron transfer in the D235N mutant may be taken as additional evidence supporting the mechanism given in Scheme 3. With the exception of W191F and D235N, the Class A mutants had nearly the same k_4 values as the CcP parent, even though the stability of CMPI is severely compromised in most of them. In class B, the k_4 value of the H181G mutant was about 50% that of the CcP parent for the complex with Ru-27-CC, while the other mutants had relatively small effects. In class C, the charge mutant D34N had the largest effect, with a k_4 value over twice as large as that of the CcP parent for the complex with Ru-27-CC.

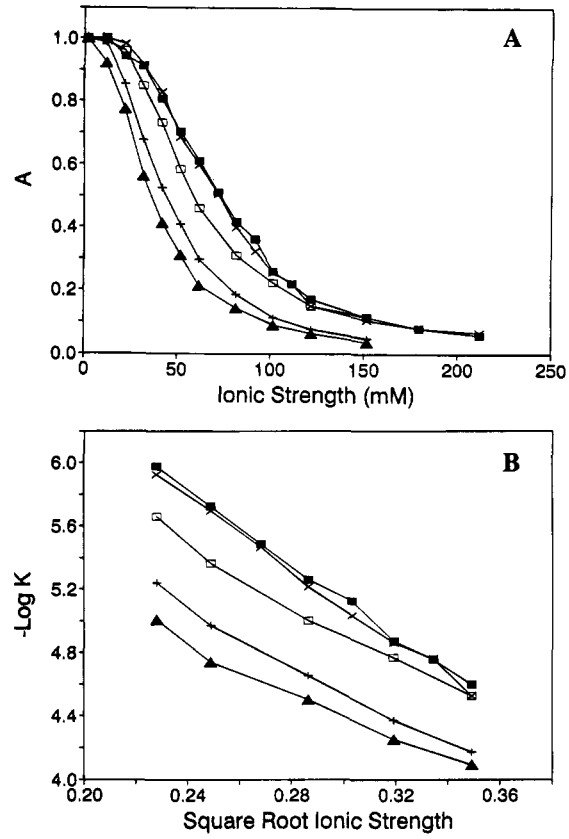

FIGURE 6: Effect of ionic strength on the reactions between Ru-27-CC and CcP mutants. Solutions contained 5 μM Ru-27-CC and 6 μM CcP mutant in 2 mM sodium phosphate, pH 6, and 0–200 mM NaCl. (A) The value of A_o was measured with the dye laser instrument as a function of ionic strength. The parameter $A = A_o/A_{ot}$, where A_{ot} is the limiting value of A_o at high concentrations of CcP and 2 mM ionic strength. (B) The value of K (in M units) was measured from eq 5, assuming that the value of A_{ot} was independent of ionic strength, and plotted as a function of the square root of ionic strength (in M units). (■) CcP; (□) E32Q; (▲) E290N; (×) E291Q; (+) A193F.

Effect of Ionic Strength on Photoinduced Electron Transfer between Ru-CC and CcP. The effect of ionic strength on the photoinduced electron-transfer reaction was rather unusual. As the ionic strength was increased in a solution containing 5 μM Ru-27-CC and 6 μM CcP, the amplitude A_o of the transient observed in the dye laser instrument decreased progressively until essentially no transient was observed above 200 mM ionic strength (Figure 6). The rapid transients observed at 200 mM ionic strength in the YAG instrument were the same as that of Ru-27-CC in the absence of CcP. These results are consistent with dissociation of the complex between Ru-27-CC and CcP. Similar results were observed for solutions containing 5 μM Ru-27-CC and 6 μM CcP(E290N), except that A_o decreased more rapidly with increasing ionic strength, indicating weaker binding (Figure 6). At intermediate ionic strength, the transients observed in the dye laser instrument were biphasic, with a fast phase with rate constant k_f and amplitude A_f and a very slow phase with rate constant k_s (Figure 7). The fraction of the reoxidation of Fe(II) due to the fast phase, A_f/A_o, decreased with increasing ionic strength, while the fraction of the slow phase increased (Table 3). The value of the fast phase rate constant k_f actually increased with increasing ionic strength for both CcP and CcP(E290N) (Table 3). The value of k_f was independent of protein concentration at a given

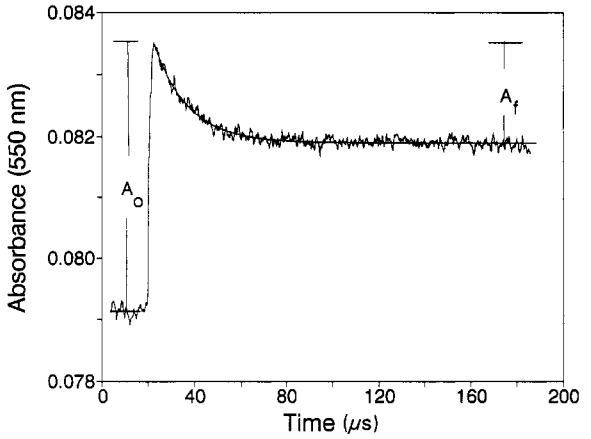

FIGURE 7: Reaction between Ru-27-CC and CcP(E290N) at 42 mM ionic strength. The solution contained 5 μM Ru-27-CC and 6 μM CcP(E290N) in 2 mM phosphate, pH 6, and 40 mM NaCl. The solution was excited in the dye laser instrument. The 550-nm absorbance transient is the average of 10 transients. The solid line is the best fit to a single exponential with $k_f = 6.7 \times 10^4$ s^{-1}, and $A_f/A_o = 0.38$. The rate constant of the slow phase was 160 s^{-1} under these conditions.

Table 3: Effect of Ionic Strength on Electron Transfer between Ru-27-CC and CcP or CcP(E290N)[a]

	CcP				E290N CcP			
I	A_o/A_f	k_f	k_4	k_5	A_o/A_f	k_f	k_4	k_5
2	0.98	62	61	<1	0.88	46	40	6
12	0.95	66	63	1−4	0.78	48	38	10
22	0.94	73	69	1−4	0.66	54	36	18
32	0.94	70	66	2−5	0.50	58	29	29
42	0.91	74	67	7	0.38	67	25	42
52	0.81	76	62	14	0.32	84	27	57
62	0.73	78	57	21	0.27	89	24	65
82	0.67	93	62	31				

[a] Solutions containing 5 μM Ru-27-CC and 6 μM CcP or CcP(E290N) in 2 mM sodium phosphate, pH 6, and 0−200 mM sodium phosphate were photoexcited in the dye laser instrument. The fast phase of the kinetics was fitted to a single exponential with rate constant k_f and amplitude A_f. The values of k_4 and k_5 were determined from the relations $k_f = k_4 + k_5$ and $A_f/A_o = k_4/(k_4 + k_5)$. The ionic strength I is in units of mM, and the rate constants are in 10^3 s^{-1}. The errors in A_o/A_f are ±0.03, and the errors in the rate constants are ±20% except where noted.

ionic strength, while the value of k_s was dependent on protein concentration, but was less than 200 s^{-1} under all conditions.

The ionic strength dependence of the kinetics is consistent with Scheme 4, where E and E• represent resting state CcP and the radical form CMPII(III,R•), respectively. At low ionic strength, the CC(III):E complex will be fully formed, and a laser light flash will rapidly lead to the reduction of the heme and the oxidation of Trp-191, resulting in formation of CC(II):E•. This corresponds to the first three steps of Scheme 3, and is complete in less than 1 μs. Intracomplex electron transfer from the heme in Ru-27-CC to the radical in E• will then lead to formation of CC(III):E. At low ionic strength, the rate constant k_5 for dissociation of CC(II):E• is expected to be much slower than k_4 and will not affect the kinetics. As the ionic strength is increased, the dissociation rate constant k_5 will increase and become competitive with k_4, resulting in dissociation of a significant fraction of CC(II):E• before electron transfer can occur. This will result in a decrease in the amplitude A_f of the fast phase and an increase in the apparent rate constant k_f for the fast phase, since k_f will be equal to the sum of k_4 and k_5. The fraction

Scheme 4

$$\begin{array}{lcl} \text{CC(II):E}^\bullet & \overset{k_5}{\underset{k_6}{\rightleftarrows}} & \text{CC(II)} + \text{E}^\bullet \\ h\nu\uparrow\downarrow k_4 & & \\ \text{CC(III):E} & \overset{k_7}{\underset{k_8}{\rightleftarrows}} & \text{CC(III)} + \text{E} \\ \text{CC(II):E} & \overset{k_9}{\underset{k_{10}}{\rightleftarrows}} & \text{CC(II)} + \text{E} \\ \text{CC(III):E}^\bullet & \overset{k_{11}}{\underset{k_{12}}{\rightleftarrows}} & \text{CC(III)} + \text{E}^\bullet \end{array}$$

of CC(II):E• that does dissociate will lead to the rebinding of CC(II) and E• with E and CC(III) to form the nonproductive complexes CC(II):E and CC(III):E•. Since the fraction of CC(II):E• initially formed by the laser flash is only about 5% of the total amount of CC(III):E, nearly all of the CC(II):E• that dissociates will rebind to form these nonproductive complexes. The reformation of the productive CC(II):E• complex from the nonproductive CC(II):E and CC(III):E• complexes will be a very slow process, accounting for the slow phase in the 550-nm transient.

The complete 550-nm transients at each ionic strength were fitted to Scheme 4 using the relations $k_f = k_4 + k_5$ and $A_f/A_o = k_4/(k_4 + k_5)$, which are valid for the present case where the rebinding of dissociated CC(II) and E• to form the productive CC(II):E• complex is very slow compared to k_4 and k_5. The electron-transfer rate constant k_4 for the Ru-27-CC:CcP complex remained approximately the same as the ionic strength was increased from 2 to 82 mM, while the dissociation rate constant k_5 increased from less than 1 $\times 10^3$ to 3.1 $\times 10^4$ s^{-1} (Table 3). The rate constant k_5 for the complex between Ru-27-CC and CcP(E290N) increased more rapidly with ionic strength than that for the CcP complex, indicating weaker electrostatic interactions (Table 3). Fitting the slow phase of the transients was less definitive, since this phase depends on all the rate constants k_5−k_{12} in Scheme 4. Good fits were obtained by assuming that the dissociation rate constants k_7, k_9, and k_{11} were each the same as k_5 and that the formation rate constants k_6, k_8, k_{10}, and k_{12} were each 1 $\times 10^9$ M^{-1} s^{-1}, which is close to the diffusion limit. However, this assumption is probably not strictly valid, and the fits are certainly not unique.

In order to further test Scheme 4, the kinetics were studied as a function of CcP concentration at a fixed Ru-27-CC concentration of 3.8 μM and an intermediate ionic strength of 50 mM (Figure 8). The value of A_o increased hyperbolically with CcP concentration, but the ratio A_f/A_o and the rate constant k_f remained constant. This behavior is consistent with Scheme 4, and indicates that A_o is proportional to the concentration of the CC(III):E complex immediately before the laser flash. The data were fit to the binding equation:

$$A_o/A_{ot} = \{K + C_o + E_o - [(K + C_o + E_o)^2 - 4C_oE_o]^{1/2}\}/2C_o \quad (5)$$

where K is the dissociation constant of the CC(III):E complex, A_{ot} is the value of A_o for the fully formed complex,

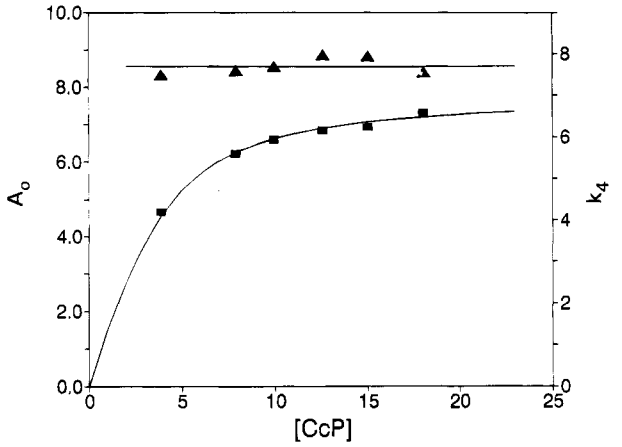

FIGURE 8: Concentration dependence of photoinduced electron transfer between Ru-27-CC and CcP. Solutions containing 3.8 μM Ru-27-CC and 3.8−21 μM CcP in 2 mM sodium phosphate, pH 6, and 50 mM NaCl were photoexcited in the dye laser instrument. The values of A_o (■) are given in units of 10^{-3} AU, and the values of k_f (▲) are given in units of 10^4 s^{-1}. The smooth line in the plot of A_o is the best fit to eq 5, with $K = 1.2$ μM. The value of A_f/A_o remained constant at 0.81 ± 0.02 for the entire concentration range.

Table 4: Electron Transfer and Dissociation Rate Constants for Complexes between Ru-27-CC and CcP Charge Mutants at 32 mM Ionic Strength[a]

mutant	k_4	k_5
CcP(MI)	66	2−5
E32Q	100	12
E34N	>100	>30
E35Q	98	17
E290N	29	29
E291Q	65	4−6
A193F	30	30

[a] The rate constants k_4 and k_5 were measured as described in Table 3 in buffers containing 2 mM sodium phosphate, pH 6, and 30 mM NaCl. The rate constants are in units of 10^3 s^{-1}, and the error limits are ±20%.

and C_o and E_o are the total concentrations of CC and E, respectively. The data of Figure 6 were fitted to eq 5 with $K = 1.2$ μM at 50 mM ionic strength. The value of A_{ot} was independent of ionic strength from 5 to 50 mM ionic strength, but it was not measured at higher ionic strength because of the very high CcP concentrations that would be required. If it is assumed that A_{ot} is independent of ionic strength over the entire range, then the ratio $A = A_o/A_{ot}$ in Figure 6A can be used to estimate the value of K as a function of ionic strength from eq 5. The value of K for the CcP complex increases from 1.2 to 25 μM as the ionic strength is increased from 50 to 120 mM, while the value for CcP(E290N) increases from 10 to 81 μM (Figure 6B).

The ionic strength dependence of the reactions of Ru-27-CC with the other CcP binding domain mutants was also studied (Figure 6; Table 4). The K value of the A193F mutant was about 5-fold larger than that for the CcP control at ionic strengths from 50 to 100 mM, while the K values of the E32Q and E291Q mutants were more similar to that of CcP (Figure 6). The values of k_5 at 30 mM ionic strength were significantly larger for the E32Q, E34N, E35N, E290N, and A193F mutants than for the parent CcP, while k_5 for E291Q was the same as that of CcP (Table 4). The A_o value for the E34N mutant decreased so rapidly with increasing ionic strength, and k_5 increased so rapidly, that reliable rate constants could not be measured at ionic strengths of 30 mM and above. The value of k_5 was estimated to be greater than 3×10^4 s^{-1} at 30 mM ionic strength.

DISCUSSION

Mechanism of Photoinduced Electron Transfer in Ru-CC:CcP Complexes. The mechanism for photoinduced electron transfer in the Ru-CC:CcP complexes shown in Scheme 3 represents a novel use of the redox chemistry of Ru(bipyridine)$_3$. The photoredox properties of Ru are used twice, first to reduce the heme on CC(III) and then to oxidize the Trp-191 indole group to a radical. The excited state Ru(II*) is a strong reducing agent with a redox potential of −0.84 V for the Ru(II*)/Ru(II) couple, and it rapidly transfers an electron to the heme of Ru-CC(III) to form Fe(II) and Ru(III). The resulting Ru(III) is a strong oxidant with a redox potential of 1.3 V for the Ru(III)/Ru(II) couple, and it oxidizes the indole group of Trp-191 to an indolyl radical in the state CMPII(III,R•). The final electron-transfer reaction from CC(II) to the indolyl radical on Trp-191 is essentially the same reaction observed in the reduction of the radical in CMPI(IV,R•) by CC(II). The photoinduced electron-transfer reaction in Scheme 3 has several unique advantages for the study of cytochrome *c* peroxidase. The reaction between CC(II) and the radical can be measured in the absence of H_2O_2 without preparing CMPI. This could potentially allow the study of electron transfer at low temperatures in frozen glasses, or even in crystalline complexes of CcP and CC. In addition, the electron-transfer properties of the radical can be studied in CcP mutants for which the CMPI species is too unstable for normal techniques. The photoinduced electron-transfer cycle could be repeated thousands of times with no apparent photolytic damage to CcP or Ru-CC, indicating the good stability of the system.

The intracomplex electron-transfer reaction was only observed for Ru-CC derivatives labeled at lysines 13, 27, and 72, which are within or close to the Pelletier−Kraut interaction domain (Figure 9). Ru-CC derivatives modified at lysine 8, 25, 39, 55, or 60 remote from the binding domain did not exhibit intracomplex electron transfer with CcP, indicating that the ruthenium complex must be in direct contact with the surface of CcP. Several observations suggest that the binding orientation of Ru-27-CC to CcP is similar to that involving native horse CC. First, the second-order rate constant for the reaction between Ru-27-CC and the radical in CMPI is actually 2-fold larger than that of native horse CC at high ionic strength (Hahm et al., 1992). Second, the effects of the CcP surface mutations on the binding interaction of Ru-27-CC (Table 4; Figure 6) parallel the effect of these mutations on the bimolecular rate constants for the reaction of native horse CC with CMPI (Miller et al., 1994b). Although no structure for a Ru-CC:CcP complex has yet been determined, the position of the Ru label can be modeled using the structure of the horse CC:CcP complex as a starting point (Figure 9). An Ru label attached through N_ϵ of Lys-27 can be placed in van der Waals contact with the methyl side chain of Ala-193 without perturbing the interface of the crystalline horse CC:CcP complex (Figure 9). In this position, the distance from the closest atom of the Ru label to Ala-193 CB is about 4 Å, and to Trp-191 CB it is about 10 Å. This would provide a very efficient pathway for electron transfer between Ru(III) and the indole group of Trp-191, consistent with the rate constant $k_3 = 7$

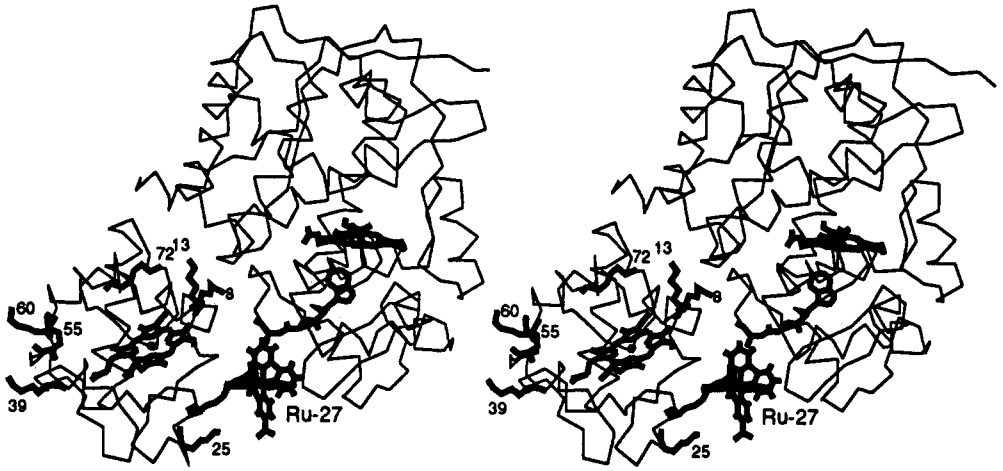

FIGURE 9: Stereo pair showing the α-carbon trace of the crystalline complex between horse CC and CcP(MI) (Pelletier & Kraut, 1992). The lysine side chains of CC are shown in bold, as are the hemes and residues 191−193 of CcP(MI). A model of the Ru label was attached to N_ϵ of Lys-27, and the conformation of the Ru-Lys-27 group was adjusted manually using the graphics program to place the Ru label in van der Waals contact with the methyl side chain of Ala-193 without causing any steric problems at the complex interface. The conformation of this residue is strictly hypothetical.

$\times 10^6$ s^{-1} for this reaction. The redox potential for the indolyl radical on Trp-191 has not been measured directly. However, Miller et al. (1994a) have presented evidence that the indolyl radical cation on Trp-191 is electrostatically stabilized by the backbone carbonyl oxygen atoms of residues 175 and 177, the heme propionates, and the carboxylate side chain of Asp-235. They estimate that the redox potential of the Trp-191 indolyl radical cation is about 0.65 V, which is stabilized by 0.35 V relative to a Trp radical in solution. Using this estimate, the driving force for the electron-transfer reaction between the indole of Trp-191 and Ru(III) would be 0.65 V. This driving force is about the same as the reorganization energy for electron transfer in many proteins (Moser et al., 1992) and would allow a maximum rate of electron transfer for this reaction.

The value of $k_4 = 6.1 \times 10^4$ s^{-1} for electron transfer from Fe(II) of Ru-27-CC to the Trp-191 indolyl radical in CMPII-(III,R•) is 2 orders of magnitude smaller than the value of k_3 for electron transfer between Ru(III) and the Trp-191 indole. This is consistent with the crystal structure of the horse CC:CcP complex (Figure 9), which revealed that the closest distance between the heme methyl group CBC of horse CC and the Ala-193-Ala-194 loop of CcP is about 7 Å (Pelletier & Kraut, 1992). This relatively large gap between the edge of the heme group of horse CC and the residues on the surface of CcP that provide the pathway for electron transfer to the Trp-191 indolyl radical would significantly decrease the rate of electron transfer. This gap is closed in the yeast CC:CcP complex, where the heme methyl group CBC is in van der Waals contact with the Ala-193-Ala-194 loop (Pelletier and Kraut, 1992). Studies in our lab have indicated that the rate constant for electron transfer from yeast CC to the Trp-191 indolyl radical in CMPI is much faster than 10^5 s^{-1} (Geren et al., 1991).

Lysines 13 and 72 are located within the Pelletier−Kraut interaction domain, and an Ru label cannot be accommodated at these residues without significantly altering the binding orientation from that observed in the crystalline horse CC:CcP complex (Figure 9). The k_4 values for Ru-13-CC and Ru-72-CC are much less than the value for Ru-27-CC, consistent with such an alteration of the binding orientation. The fact that the reaction between Ru(III) and the Trp-191 indole group is observed with these derivatives indicates that the binding orientation places the Ru label fairly close to the CcP surface residues leading to Trp-191. The k_4 values for all three derivatives are quite similar to the values of k_{etf} for electron transfer to the radical in CMPI(IV,R•) (Table 2). This suggests that there are no significant differences in the binding orientations of the Ru-CC derivatives to the two redox forms of the peroxidase.

Photoinduced Electron Transfer between Ru-CC and CcP Mutants Altered at the Heme Crevice or at Aromatic Residues. One of the major advantages of the present technique is that it allows measurement of electron transfer to the radical without having to use H_2O_2 to form CMPI. This has allowed us to measure electron transfer in a number of CcP mutants in which CMPI is unstable. Among the heme crevice mutants, no photoinduced intracomplex electron-transfer reaction was observed in W191F or D235N. Asp-235 forms hydrogen bonds to both Trp-191 and His-175, the proximal heme ligand (Wang et al., 1990). Mutation of Asp-235 to Asn disrupts both of these hydrogen bonds and causes the indole side chain of Trp-191 to flip over (Wang et al., 1990). The D235N mutant has no enzymatic activity, and although the heme is oxidized to an oxyferryl state by H_2O_2, there is no oxidation of the Trp-191 indole to a radical cation (Miller et al., 1992; Vitello et al., 1992; Goodin & McRee, 1993). These results suggest that the negative charge on the carboxylate of Asp-235 as well as the hydrogen bond network stabilize the indolyl radical cation on Trp-191. Removal of the negative charge and disruption of the hydrogen bond network would be expected to increase the redox potential of the indole group and prevent its oxidation by Ru(III), consistent with the present results. The sulfur atoms of Met-230 and Met-231 are each about 4.5 Å from $N^{\epsilon 1}$ of the indole group of Trp-191 and are thought to stabilize the radical by decreasing its redox potential (Edwards et al., 1987; Fishel et al., 1991). CMPI can be formed in both the M230I and M231L mutants, but it is considerably less stable than for the native enzyme, particularly in the case of M231L (Fishel et al., 1991). Liu et al. (1994) have shown that the M230I mutation substantially decreases the rate of electron transfer from Trp-191 to the heme oxyferryl center (reaction 2 of Scheme 1), consistent with an alteration

of the stability of the radical. In the present studies, photoinduced electron transfer was observed in complexes with both M230I and M231L, indicating that the electron-transfer properties of the radical with Ru-CC are not greatly perturbed (Table 2).

Arg-48 and His-52 are on the distal side of the heme pocket and are involved in the formation of CMPI. His-52 has been proposed to accept a proton from the incoming H_2O_2 and to assist the binding of the peroxide anion to the heme Fe(III) (Erman et al., 1993). Arg-48 promotes O−O heterolysis by electrostatically stabilizing the developing negative charge on the distal oxygen (Vitello et al., 1993). Both the rate of formation of CMPI and its stability are significantly decreased in the R48K, R48L, and H52L mutants. For this reason, it was not possible to measure the rate of electron transfer from Ru-CC(II) to the radical in CMPI(IV,R$^\bullet$). However, photoinduced electron transfer in Ru-CC:CcP complexes involving these mutants was readily observed (Table 1). The k_4 rate constants for the reactions of Ru-27-CC with these mutants are comparable to that for the CcP parent, while the values for the reactions of Ru-13-CC and Ru-72-CC with H52L were somewhat larger than those for the CcP parent. These changes in k_4 probably reflect subtle changes in the conformation of the complex involving the H52L mutant. Overall, these results provide evidence that the electron-transfer properties of the radical on Trp-191 are not significantly affected by these distal side mutants.

Photoinduced electron transfer was also observed in complexes between Ru-CC and a number of CcP mutants altered at surface aromatic residues that could potentially be involved in electron transfer. Tyr-39 is located on the surface of CcP within the Pelletier−Kraut binding domain, while Tyr-42 is located just outside the binding domain. Tyr-229 is the closest tyrosine to Trp-191 and is located just outside the binding domain. Trp-223 is located some distance from the Pelletier−Kraut binding domain but is close to the Poulos−Kraut (1980) binding domain. The k_4 rate constants for the Y39F, Y42F, W223F, and Y229F mutants are similar to those of the CcP parent, indicating no direct role for these aromatic residues in electron transfer from Ru-CC(II) to the radical. Although k_3 was not measured directly on the YAG laser instrument for these derivatives, the values of A_o obtained using the dye laser instrument were the same as those of the CcP parent within ±30%, indicating no significant change in the rate of oxidation of Trp-191 by Ru(III). The largest changes in k_4 were observed for the H181G mutant, with a 2-fold increase for Ru-13-CC and a 3-fold decrease for Ru-27-CC compared to the CcP control. His-181 was postulated to provide a pathway for electron transfer between the two heme groups in the Poulos−Kraut model of the CC:CcP complex. However, His-181 is important in maintaining the structural integrity of CcP (Miller et al., 1988, 1990), and replacing it with Gly decreases the stability of CMPI. The 2−3-fold changes in k_4 compared to the CcP parent are probably a result of subtle changes in the conformation of the complex.

Effect of Ionic Strength and Surface Charge Mutations on Electron Transfer in Ru-CC:CcP Complexes. The effect of ionic strength on the kinetics of electron transfer in Ru-CC:CcP complexes is consistent with Scheme 4, which postulates that the transient intermediate CC(II):E$^\bullet$ can either undergo intracomplex electron transfer to form CC(III):E with rate constant k_4 or dissociate with rate constant k_5. The equilibrium dissociation constant K of the Ru-27-CC(III):E complex is 1.2 μM at 50 mM ionic strength, increasing to 1.9 μM at 64 mM ionic strength and 14 μM at 100 mM ionic strength (Figures 6B and 8). By comparison, the value of K is 8 μM for native horse CC at 64 mM ionic strength and 13 μM for native yeast iso-1-CC at 200 mM ionic strength (Erman & Vitello, 1980; Leonard & Yonetani, 1974). Ru-27-CC thus appears to interact more strongly with CcP than horse CC, but less strongly than yeast iso-1-CC. The dissociation rate constant k_5 of the Ru-27-CC(II):E$^\bullet$ complex increases from <1000 s^{-1} at 2 mM ionic strength to 3.1×10^4 s^{-1} at 80 mM ionic strength (Table 3). Yi et al. (1994) have recently measured the dissociation rate constant for the complex of E with native yeast iso-1-CC-(III) to be 180 s^{-1} at 10 mM ionic strength. The dissociation rate constant of horse CC(III) is expected to be larger than that of yeast iso-1-CC (Moench et al., 1992), consistent with the results obtained here for the horse Ru-27-CC(II):E$^\bullet$ complex. What is unique about the present method, however, is the ability to measure the dissociation rate constant to high ionic strength where the value is quite large.

Mutation of charged residues located at the Pelletier−Kraut interaction domain has a significant effect on the ionic strength dependence of the reaction with Ru-27-CC. The dissociation constant K for the Ru-27-CC(III):E complex is increased 10-fold by the E290N mutation at 50 mM ionic strength, and more than 10-fold by the E34N mutation. The rate constant k_5 for the dissociation of the Ru-27-CC(II):E$^\bullet$ complex is increased 7-fold by the E290N mutation at 30 mM ionic strength, and more than 10-fold by the E34N mutation (Table 4). The E32Q and E35N mutations have smaller effects on K and k_5, while the E291Q mutation has no effect on either parameter (Figure 6; Table 4). These results indicate that Asp-34, Glu-35, and Glu-290 have important roles in stabilizing the Ru-27-CC(III):E and Ru-27-CC(II):E$^\bullet$ complexes, and suggest that the binding orientation is similar to that in the horse CC:CcP crystal structure (Pelletier & Kraut, 1992). In the crystal structure, the carboxylate oxygen atoms of Glu-35 and Glu-290 are hydrogen bonded to amino groups of CC lysines 87 and 72, respectively, while Asp-34 is quite close to lysine 72. The oxygen atoms of Glu-32 and Glu-291 are about 5 and 8 Å, respectively, from the nearest complementary lysine amino groups on CC, consistent with the smaller effects on K and k_5 by the E32Q and E291Q mutations. Ala-193 is at the center of the Pelletier−Kraut interaction domain, and introduction of a bulky phenyl group in the A193F mutant is expected to lead to a decrease in the stability of the complex, consistent with the effects on K and k_5 (Figure 6; Table 4). Miller et al. (1994b) have found that the effects of these interaction domain mutations on the bimolecular rate constants for the reactions of native horse and yeast CC with the radical in CMPI at high ionic strength closely parallel the effects on K observed in the present experiments at comparable ionic strengths.

The D34N mutation has the largest effect on the rate constant k_4 for electron transfer in the Ru-27-CC(II):E$^\bullet$ complex at low ionic strength, increasing it from 6.1×10^4 to 1.3×10^5 s^{-1} (Table 2). This indicates that the D34N mutation leads to a change in the binding orientation of the Ru-27-CC(II):E$^\bullet$ complex. There is also a significant difference between the values of k_4 and k_{etf} for the reaction of

Ru-27-CC with the D34N mutant (Table 2). This probably reflects a difference between the orientation of Ru-27-CC binding to the two redox forms of the enzyme, CMPI(IV,R•) and CMPII(III,R•). It is interesting that the largest differences between k_4 and k_{etf} are observed for the surface mutants D34N, E35Q, E290N, and A193F located within or close to the interaction domain (Table 2). These mutants have the weakest binding energies and would be expected to be the most sensitive to subtle conformational effects which could lead to differences in the binding orientations of Ru-CC to the two redox forms of the peroxidase. The difference in binding orientation could be quite small, since an increase of only 0.5 Å in the distance for electron transfer is predicted to lead to a 2-fold decrease in the rate constant for a typical protein system (Moser et al., 1992).

ACKNOWLEDGMENT

The authors thank Seong Park and Thi Ho for excellent technical assistance.

REFERENCES

Coulson, A. F. W., Erman, J. E., & Yonetani, T. (1971) *J. Biol. Chem. 246,* 917−924.
Durham, B., Pan, L. P., Long, J., & Millett, F. (1989) *Biochemistry 28,* 8659−8665.
Edwards, S. L., Xuong, N. H., Hamlin, R. C., & Kraut, J. (1987) *Biochemistry 26,* 1503−1511.
Erman, J. E., & Vitello, L. B. (1980) *J. Biol. Chem. 255,* 6224−6227.
Erman, J. E., Vitello, L. B., Mauro, J. M., & Kraut, J. (1989) *Biochemistry 28,* 7992−7995.
Erman, J. E., Vitello, L. B., Miller, M. A., Shaw, A., Brown, K. A., & Kraut, J. (1993) *Biochemistry 32,* 9798−9806.
Finzel, B. C., Poulos, T. L., & Kraut, J. (1984) *J. Biol. Chem. 259,* 13027−13036.
Fishel, L. A., Villafranca, J. E., Mauro, J. M., & Kraut, J. (1987) *Biochemistry 26,* 351−360.
Fishel, L. A., Farnum, M. F., Mauro, J. M., Miller, M. A., Kraut, J., Liu, Y., Tan, X., & Scholes, C. P. (1991) *Biochemistry 30,* 1986−1996.
Geren, L. M., Hahm, S., Durham, B., & Millett, F. (1991) *Biochemistry 30,* 9450−9457.
Goodin, D. B., & McRee, D. E. (1993) *Biochemistry 32,* 3313−3324.
Goodin, D. B., Mauk, A. G., & Smith, M. (1987) *J. Biol. Chem. 262,* 7719−7724.
Hahm, S., Durham, B., & Millett, F. (1992) *Biochemistry 31,* 3472−3477.
Hahm, S., Geren, L., Durham, B., & Millett, F. (1993) *J. Am. Chem. Soc. 115,* 3372−3373.
Hahm, S., Miller, M. A., Geren, L., Kraut, J., Durham, B., & Millett, F. (1994) *Biochemistry 33,* 1473−1480.
Hazzard, J. T., & Tollin, G. (1991) *J. Am. Chem. Soc. 113,* 8956−8957.
Hazzard, J. T., Poulos, T., & Tollin, G. (1987) *Biochemistry 26,* 2836−2848.
Hazzard, J. T., McLendon, G., Cusanovich, M. A., & Tollin, G. (1988a) *Biochem. Biophys. Res. Commun. 151,* 429−434.
Hazzard, J. T., Moench, S. J., Erman, J. E., Satterlee, J. D., & Tollin, G. (1988b) *Biochemistry 27,* 2002−2008.
Hazzard, J. T., McLendon, G., Cusanovich, M. A., Das, G., Sherman, F., & Tollin, G. (1988c) *Biochemistry 27,* 4445−4451.
Ho, P. S., Hoffman, B. M., Kang, C. H., & Margoliash, E. (1983) *J. Biol. Chem. 258,* 4356−4363.
Houseman, A. L. P., Doan, P. D., Goodin, D. B., & Hoffman, B. M. (1993) *Biochemistry 32,* 4430−4443.
Kim, K. L., Kang, D. S., Vitello, L. B., & Erman, J. E. (1990) *Biochemistry 29,* 9150−9159.
Leonard, J. J., & Yonetani, T. (1974) *Biochemistry 13,* 1465−1468.
Liu, R.-Q., Hahm, S., Miller, M. A., Han, G. W., Geren, L., Hibdon, S., Kraut, J., Durham, B., & Millett, F. (1994) *Biochemistry 33,* 8678−8685.
Louie, G. V., & Brayer, G. D. (1990) *J. Mol. Biol. 214,* 527−555.
Mauro, J. M., Fishel, L. A., Hazzard, J. T., Meyer, T. E., Tollin, G., Cusanovich, M. A., & Kraut, J. (1988) *Biochemistry 27,* 6243−6256.
Miller, M. A., Hazzard, J. T., Mauro, J. M., Edwards, S. L., Simons, P. D., Tollin, G., & Kraut, J. (1988) *Biochemistry 27,* 9081−9088.
Miller, M. A., Mauro, J. M., Smulevich, G., Coletta, M., Kraut, J., & Traylor, T. G. (1990) *Biochemistry 29,* 9978−9988.
Miller, M. A., Bandyopadhyay, D., Mauro, J. B., Traylor, T. G., & Kraut, J. (1992) *Biochemistry 31,* 2789−2797.
Miller, M. A., Han, G. W., & Kraut, J. (1994a) *Proc. Natl. Acad. Sci. U.S.A.* (in press).
Miller, M. A., Liu, R.-Q., Hahm, S., Geren, L., Hibdon, S., Kraut, J., Durham, B., & Millett, F. (1994b) *Biochemstry 33,* 8686−8693.
Moench, S. J., Chroni, S., Lou, B.-S., Erman, J. E., & Satterlee, J. D. (1992) *Biochemistry 31,* 3661−3670.
Moser, C. C., Keske, J. M., Warncke, K., Farid, R. S., & Dutton, P. L. (1992) *Nature 355,* 796−802.
Nuevo, M. R., Chu, H.-H., Vitello, L. B., & Erman, J. E. (1993) *J. Am. Chem. Soc. 115,* 5873−5874.
Pan, L. P., Durham, B., Wolinska, J., & Millett, F. (1988) *Biochemistry 27,* 7180−7184.
Pan, L. P., Hibdon, S., Liu, R.-Q., Durham, B., & Millett, F. (1993) *Biochemistry 32,* 8492−8498.
Pelletier, H., & Kraut, J. (1992) *Science 258,* 1748−1755.
Poulos, T. L., & Kraut, J. (1980) *J. Biol. Chem. 255,* 10322−10330.
Scholes, C. P., Liu, Y., Fishel, L. A., Farnum, M. F., Mauro, J. M., & Kraut, J. (1989) *Israel J. Chem. 29,* 85−92.
Sivaraja, M., Goodin, D. B., Smith, M., & Hoffman, B. M. (1989) *Science 245,* 738−740.
Stemp, E. D. A., & Hoffman, B. M. (1993) *Biochemistry 32,* 10848−10865.
Strickland, S., Palmer, G., & Massey, B. (1975) *J. Biol. Chem. 250,* 4048−4052.
Summers, F. E., & Erman, J. E. (1988) *J. Biol. Chem. 263,* 14267−14275.
Vitello, L. B., Erman, J. E., Miller, M. A., Mauro, J. M., & Kraut, J. (1992) *Biochemistry 31,* 11524−11535.
Vitello, L. B., Erman, J. E., Miller, M. A., Wang, J., & Kraut, J. (1993) *Biochemistry 32,* 9807−9818.
Wang, J., Mauro, M., Edwards, S. L., Oatley, S. J., Fishel, L. A., Ashford, V. A., Xuong, N. H., & Kraut, J. (1990) *Biochemistry 29,* 7160−7173.
Yi, Q., Erman, J. E., & Satterlee, J. D. (1994) *J. Am. Chem. Soc. 116,* 1981−1987.
Yonetani, T., Schleyer, H., & Ehrenberg, A. (1966) *J. Biol. Chem. 241,* 3240−3243.
Zhou, J. S., & Hoffman, B. M. (1993) *J. Am. Chem. Soc. 113,* 11008−11009.
Zhou, J. S., & Hoffman, B. M. (1994) *Science 265,* 1693−1696.

BI941825M